A Role for Differential Glycoconjugation in the Emission of Phenylpropanoid Volatiles from Tomato Fruit Discovered Using a Metabolic Data Fusion Approach[1][W][OA]

Yury M. Tikunov*, Ric C.H. de Vos, Ana M. González Paramás, Robert D. Hall, and Arnaud G. Bovy

Centre for BioSystems Genomics, 6700 AB Wageningen, The Netherlands (Y.M.T., R.C.H.d.V., A.M.G.P., R.D.H., A.G.B.); Plant Research International, 6700 AA Wageningen, The Netherlands (Y.M.T., R.C.H.d.V., R.D.H., A.G.B.); Laboratory for Plant Physiology, Wageningen University, 6703 BD Wageningen, The Netherlands (Y.M.T.); and Universidad de Salamanca, Area de Nutrición y Bromatología, Facultad de Farmacia, Campus Miguel de Unamuno, E–37007 Salamanca, Spain (A.M.G.P.)

A role for differential glycoconjugation in the emission of phenylpropanoid volatiles from ripening tomato fruit (*Solanum lycopersicum*) upon fruit tissue disruption has been discovered in this study. Application of a multiinstrumental analytical platform for metabolic profiling of fruits from a diverse collection of tomato cultivars revealed that emission of three discriminatory phenylpropanoid volatiles, namely methyl salicylate, guaiacol, and eugenol, took place upon disruption of fruit tissue through cleavage of the corresponding glycoconjugates, identified putatively as hexose-pentosides. However, in certain genotypes, phenylpropanoid volatile emission was arrested due to the corresponding hexose-pentoside precursors having been converted into glycoconjugate species of a higher complexity: dihexose-pentosides and malonyl-dihexose-pentosides. This glycoside conversion was established to occur in tomato fruit during the later phases of fruit ripening and has consequently led to the inability of red fruits of these genotypes to emit key phenylpropanoid volatiles upon fruit tissue disruption. This principle of volatile emission regulation can pave the way to new strategies for controlling tomato fruit flavor and taste.

More than 7,000 metabolites, including volatiles, have already been identified in plant-based foods and beverages (Goff and Klee, 2006). Volatile organic compounds constitute a significant part of the plant metabolome, and the number of individual volatiles already described for various plants is approaching 2,000 (Dudareva et al., 2006). Significant progress has been made on the functional characterization of these plant volatiles over the past decades. For example, volatiles have been shown to play an important role in the interaction between plants and their environment. They are involved in the defense of plants against pathogens, where they serve as airborne signaling molecules to induce a defense response in other plant parts or neighboring plants (Shulaev et al., 1997). They also act as direct repellents of herbivorous pests or as attractants of the predators of these pests as part of the "cry for help" response (Dudareva et al., 2004; Kappers et al., 2005; Baldwin et al., 2006). In addition, flower volatiles are important for the attraction of pollinators (Dudareva et al., 2004), while fruit volatiles may have a role in attracting seed dispersers (Goff and Klee, 2006; Schwab et al., 2008). Besides their physiological and ecological functions, plant volatiles are also important determinants of consumer quality traits in flowers, fruits, and vegetables as well as the processed products derived from them.

Tomato (*Solanum lycopersicum*) is one of the most important vegetable crops worldwide, and its fresh fruits and processed products are consumed and appreciated in every society. Volatiles are considered as major determinants of tomato fruit flavor (Buttery et al., 1987; Buttery and Ling, 1993; Baldwin et al., 1998, 2000; Tandon et al., 2000; Krumbein et al., 2004; Ruiz et al., 2005; Tieman et al., 2006; Kovács et al., 2009; Zanor et al., 2009). Several hundred tomato fruit volatile compounds have been described in the literature (Petro-Turza, 1987), but only a small part of this diversity is believed to have an impact on tomato fruit organoleptic properties (Buttery and Ling, 1993; Baldwin et al., 2000). We have previously screened red-ripe fruits for variation in their volatile metabolome using a collection of 94 tomato cultivars representing the current diversity within commercial

germplasm (Tikunov et al., 2005). In that study, three phenylpropanoid (PhP) volatiles, methyl salicylate (MeSA), guaiacol, and eugenol, were found to be discriminatory within this germplasm collection and roughly divided the cultivars into two groups. Fruits from one group had the capacity to emit significant amounts of these three PhP volatiles upon fruit tissue disruption (blending), while fruits from the other group emitted none or hardly any.

The considered relevance of these findings relates to their potential importance in consumer perception of fruit taste differences. It has been proposed previously that PhP volatiles likely have an impact on tomato fruit aroma. MeSA, the methyl ester of salicylic acid, is a potent odor component of wintergreen (*Gaultheria procumbens*). MeSA content has been shown to be negatively correlated with typical tomato flavor (Krumbein and Auerswald, 1998). Guaiacol is also a well-known flavoring compound and has been associated with a so-called "pharmaceutical" aroma in tomato fruits (Causse et al., 2002). Likewise, eugenol is a well-known odorant that gives the distinctive, pungent flavor to cloves (*Syzygium aromaticum*) and significantly contributes to the aroma of cinnamon (*Cinnamomum verum*). Although a potential physiological role for these PhP volatiles in tomato fruits remains unclear, they have been implicated to have a signaling and/or defense function (Shulaev et al., 1997; Koeduka et al., 2006; Sasso et al., 2007). Therefore, there is clear potential for the release of these compounds to influence, either negatively or positively, tomato flavor.

In plants, PhP volatiles are primarily derived from Phe (Dudareva and Pichersky, 2000). Cinnamic acid, directly derived from Phe by a deamination catalyzed by Phe ammonia lyase, can either be β-oxidatively or nonoxidatively converted into benzoic acid. This can be further hydroxylated into salicylic acid by benzoic acid 2-hydroxylase. Recently, genetic studies in Arabidopsis (*Arabidopsis thaliana*) revealed the existence of an alternative pathway for the production of salicylic acid from isochorismate, thus bypassing Phe and its derivatives (Wildermuth et al., 2001). Salicylic acid is the immediate precursor of the volatile MeSA, through the action of salicylic acid methyl transferase (Boatright et al., 2004). Cinnamic acid can also be converted to other phenolic acids: *p*-coumaric acid, caffeic acid, and ferulic acid. Ferulic acid can be converted into coniferyl alcohol and further to eugenol (Gang, 2005). The biochemical origin of guaiacol in plants is not completely known. However, its chemical structure clearly points to the same PhP origin, as has already been demonstrated for bacteria (Chang and Kang, 2004).

Glycosylation is a common means to conjugate plant secondary metabolites, in order to facilitate their transport and storage and to reduce their reactivity by blocking reactive hydroxyl groups. In tomato fruit, many volatile compounds, including PhP volatiles, are bound as glycosides, thus representing an aroma reserve (Buttery et al., 1990; Marlatt et al., 1992; Ortiz-Serrano and Gil, 2007). Such glycosidically bound volatiles can be liberated when cell compartmentation is destroyed, as happens on consumption of fresh fruits or industrial processing or as may happen during late ripening stages. As a consequence of this disruption, the contents of different cell compartments can mix and stored volatile glycosides become exposed to endogenous or exogenous cleavage enzymes, such as glycosyl hydrolases (glycosidases), which leads to glycoside cleavage and volatile emission. Thus, understanding the biochemical processes leading to the formation and/or cleavage of volatile glycoconjugates may provide tools to exploit more efficiently the aroma reserve present in tomato fruit in order to improve tomato fruit flavor.

In order to gain greater insight into the volatile compound variation in tomato fruit, we previously analyzed the volatile metabolites using solid-phase microextraction-gas chromatography-mass spectrometry (SPME-GC-MS) in a broad screening of 94 contrasting tomato genotypes representing the variation present in the germplasm of commercial tomato varieties (Tikunov et al., 2005; Van Berloo et al., 2008). This nontargeted metabolomics approach enabled the detection and putative identification of 322 volatiles. Subsequent multivariate analysis revealed (1) differences between tomato types (cherry versus round tomatoes) driven by the accumulation of phenolic-derived volatiles such as phenylethanol and phenylacetaldehyde, and (2) that the PhP-derived volatiles MeSA, guaiacol, and eugenol roughly split the set of genotypes into two distinct groups, independent of tomato fruit (pheno)type, where fruits of one of these groups emitted considerable amounts of these three PhP volatiles but fruits of the other emitted little or none.

In this paper, we describe the investigation into the biochemical basis underlying this difference in capacity to emit PhP volatiles. A multiinstrumental metabolomics platform was used to profile fruits of the same broad tomato germplasm collection for both volatile and nonvolatile metabolites. Metabolic data fusion of both liquid chromatography (LC)-MS and GC-MS data sets, followed by multivariate analyses, suggested a principle for the regulation of PhP volatile emission in tomato fruit through differential volatile-sugar conjugation patterns. Subsequent series of quantitative biochemical experiments proved an important role of this process in regulating the emission of PhP volatiles from tomato fruit.

RESULTS

Approach to Elucidate Pathways Leading to Flavor-Related Volatiles in Tomato

Volatile metabolites are generally produced from nonvolatile precursors. In order to get more insight

into the regulation and dynamics of volatile biosynthesis pathways in tomato fruit, we aimed to compare the metabolite profiles of volatile compounds with those of nonvolatile compounds by analyzing and comparing the fruit metabolic composition of fruit materials of differing origin: a major sample set of 94 cultivars; a number of in vitro enzymatic assays; and a multigenotypic fruit-ripening series. Both GC-MS (volatiles) and LC-quadrupole time-of-flight (QTOF)-MS (nonvolatile, semipolar compounds) approaches were used. The fruits analyzed were from the same collection of 94 contrasting tomato genotypes as described previously, grown in a replicate trial (Tikunov et al., 2005).

Volatile metabolites were analyzed using head space SPME-GC-MS. Our sample preparation procedure involved a thawing of initially frozen ground tomato fruits for 10 min at 30°C prior to analysis. This allows the action of endogenous fruit enzymes that are induced, activated, or brought into contact with their substrates upon breakdown of cell compartmentation and is meant to resemble processes induced upon fruit blending, a term used further in the text as a simplified reference to the procedure. After sample analysis, the GC-MS chromatograms were subjected to full mass spectral alignment using MetAlign software (www. metalign.nl) followed by the filtering out of low-intensity ion fragments. Multiple mass signals derived from the same compound were grouped according to the in-house-developed Multivariate Mass Spectral Reconstruction (MMSR) software, as described previously (Tikunov et al., 2005), which resulted in the detection of 217 volatiles each containing more than five fragment ions in their mass spectrum. The volatiles detected and putatively identified on the basis of their fragment masses are listed in Supplemental Table S1. The identities and intergenotypic profiles of 42 volatiles, including MeSA, guaiacol, and eugenol, confirmed the results obtained in our previous trial (Tikunov et al., 2005).

Semipolar, nonvolatile metabolites were analyzed by LC-QTOF-MS of methanolic extracts from the same tomato fruit samples. In contrast to the procedure used for the detection of volatiles, the methanolic extracts were directly prepared from frozen fruit powder without any prior incubation or thawing. Thus, since fruits were frozen in liquid nitrogen within a few seconds and stored at −80°C before analysis, sample composition resembles the metabolic composition of intact tomato fruit. Like the GC-MS chromatograms, the LC-MS chromatograms were subjected to full mass spectral alignment using the MetAlign software package followed by filtering out of low-intensity ion fragments. This revealed a data matrix of 1,415 ion fragments × 94 samples analyzed. The MMSR performed on this data set resulted in 386 ion fragment clusters, predicted to represent 386 different compounds. The most abundant ion fragment within each cluster was selected as representative of each compound and was used for further analyses. Individuals in this large group of putative compounds were not subjected to prior identification and were thus initially treated as unknowns.
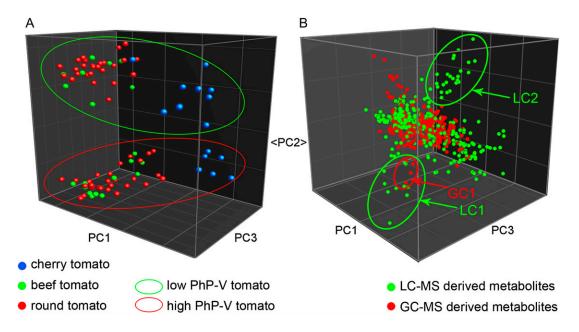
Fusion of Volatile and Nonvolatile Data

In order to find correlations between volatile and nonvolatile metabolites, low-level data fusion was performed by concatenation of both LC-MS and GC-MS normalized data sets. This resulted in a data matrix of 94 genotypes × 603 putative metabolites. A principal components analysis was performed on the fused data set (Fig. 1). The genotype clustering obtained was similar to that observed previously using GC-MS data only (Tikunov et al., 2005): the first principal component (PC1) revealed differences determined by tomato type (i.e. cherry versus the rest) and described 17.6% of the variation in the data, while the second principal component (PC2) divided the genotype set into two distinct groups independent of tomato type (Fig. 1A). This dichotomy described 16.4% of the total data variation and was determined to be primarily linked to the ability/inability to emit PhP-derived volatiles, such as MeSA, guaiacol, and eugenol (Fig. 1B, group GC1). In the fused data set, these three volatile compounds were clearly observed to be associated with a number of LC-MS-detected compounds (Fig. 1B, group LC1). In addition, another group of LC-MS derived compounds appeared as the second determinant of PC2 and showed a negative correlation with the PhP volatiles and their cocorrelating nonvolatile compounds (Fig. 1B, group LC2). According to the Student's t test performed, metabolites of all three groups (GC1, LC1, and LC2) were significantly different ($P < 0.00001$) between the fruit groups differentiated by PC2 (Fig. 1A).

The fusion of GC-MS and LC-MS data has identified two distinct genotypic groups. One group was able to emit PhP volatiles from blended fruit tissue and showed a high abundance of the nonvolatile compounds belonging to the LC1 group and the complete absence of compounds belonging to the LC2 group. The other group had an abundance of nonvolatile compounds of the LC2 group, while PhP volatiles and the LC1 nonvolatile compounds were virtually absent. To address a possible relationship between these metabolites, the correlating nonvolatile compounds were subjected to further identification.

PhP Volatile Emission Correlates with the Presence of Corresponding PhP Volatile Hexose-Pentosides

In order to shed light on the identity of the nonvolatile compounds correlating with the known PhP volatiles, the LC-MS signals of the putative compounds belonging to the LC1 group were analyzed in more detail. Eugenol, as measured by GC-MS, revealed the strongest correlation ($r = 0.8$; $P < 0.00001$) to the nonvolatile compound LC1.1 of the LC1 group (eluting at retention time 29.52 min and

Figure 1. Principal components analysis of the LC-MS/GC-MS fused data obtained from 94 contrasting tomato genotypes. A, Clustering of tomato genotypes along the first three principal components (PC): PC1, PC2, and PC3 describe 17.6%, 16.4%, and 9.0% of the total metabolic variation in fruits of the 94 tomato cultivars. B, Clustering of volatile and nonvolatile compounds determining the genotype structure shown in A. Fruit type-independent clustering of genotypes (A, red and green circles) along PC2 was determined by the three groups of compounds shown: one group of volatile compounds detected by GC-MS (GC1), consisting of the PhP volatiles MeSA, guaiacol, and eugenol (GC1 group); and two groups of nonvolatile compounds detected by LC-MS, LC1 and LC2. The GC1 and LC1 compounds showed a high abundance in high-PhP volatile (PhP-V) genotypes (A, red circles), and LC2 compounds showed higher abundance in low-PhP volatile genotypes (A, green circles).

with a selective nominal ion fragment of mass-to-charge ratio [m/z] 503; Table I). According to MMSR results, this m/z 503 was found to correlate strongly with several other ions, of which m/z 457 and m/z 293 were the most abundant (Table I). By applying accurate mass calculations and LC-MS/MS on selected ions, mass 503 (observed accurate m/z = 503.1747) appeared to be the formic acid adduct (FA; mass 46.0055) of the ion with m/z 457 (observed mass 457.1709). Subtraction of correlating fragment m/z 293 (accurate mass 293.0868) from selected ion m/z 457 gave a neutral mass loss of 164.0841. This corresponds closely to the molecular mass of eugenol (-2.4 ppm deviation from calculated mass). Indeed, a fragment ion with an accurate mass of 163.0766, corresponding to within 1 ppm of that of eugenol ([M – H]$^-$ = 163.0765), was detected using LC-MS/MS. These results suggest that compound LC1.1 represents a conjugated form of eugenol. The same calculations and identification strategies were performed on the remaining two compounds, LC1.2 and LC1.3 (Table I), which each also correlated strongly with a PhP volatile. This resulted in two mass spectral models similar to LC1.1: (1) compound LC1.2 eluting at 19.25 min represents a MeSA conjugate (LC1.2 correlated with m/z 491 and m/z 293; application of the above fragmentation analysis model gave m/z 491 – m/z 46 [FA] = m/z 445 – m/z 293 = 152 = the molecular mass of MeSA); (2) compound LC1.3 eluting at 16.22 min represents a

guaiacol conjugate (m/z 463 – m/z 46 [FA] = m/z 417 – m/z 293 = m/z 124 = the molecular mass of guaiacol). These results suggest that the three compounds detected by LC-MS, correlating to the three PhP volatiles, represented their respective conjugates, each modified in a similar way with a linkage to a fragment of m/z 293. The observed exact masses, ranging from 293.0868 to 293.0884, have on average a 2.1-ppm deviation from the elemental composition $C_{11}H_{18}O_9$. This fragment ion, therefore, appears to be a hexose-pentose diglycosidic moiety: [(hexose – H_2O) + (pentose – H_2O)]$^-$. Indeed, in some MS/MS experiments, we could also observe the corresponding hexose and pentose fragments with m/z 162 and 132 (low abundances of these ions did not allow accurate mass calculation), respectively (data not shown). None of the remaining compounds of the LC1 group revealed any relation to guaiacol, MeSA, or eugenol according to MS and MS/MS fragmentation patterns.

Low-PhP Volatile Tomato Fruits Contain PhP Volatiles Bound as Complex Triglycosides

The group of genotypes whose fruits did not emit PhP volatiles upon blending and did not contain the corresponding hexose-pentosides had significant amounts of nonvolatile compounds of the LC2 group from the LC-MS data set (Fig. 1). To shed light on their possible structure, these compounds were also further

Table I. *LC-QTOF-MS and LC-QTOF-MS/MS analysis of nonvolatile compounds correlating with PhP volatiles*

Column 1 represents the identifier (ID) of an ion fragment cluster derived by MMSR clustering, representing putative semipolar nonvolatile compounds, detected by LC-MS. The retention time (min) of these putative compounds is indicated in column 2. Column 3 shows the identity of the volatile compounds correlated with the putative nonvolatile compounds and the corresponding Pearson product correlation coefficients (*r*). nd, Not detected. Mass spectra of the nonvolatile compounds and ion fragments of these mass spectra selected for MS/MS analyses are shown in columns 4 and 5, respectively. Ion fragments observed in MS/MS analyses are listed in column 6, and the next four columns represent putative identification results of the observed ion fragments: calculated masses of the elemental formulas predicted (column 7) and their deviations from the observed masses in ppm (column 8), elemental formulas predicted for the observed ion fragments (column 9), and, finally, putative identities of the observed masses (column 10).

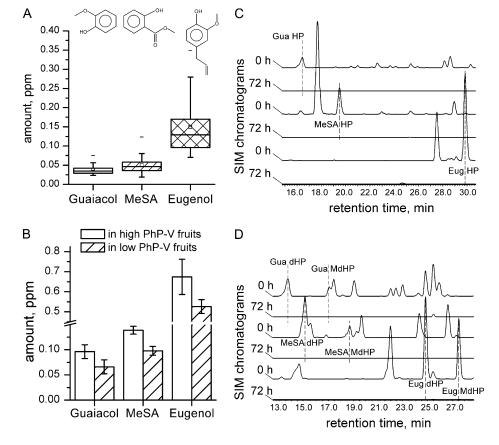| LC-QTOF-MS and MMSR Ion Clustering				LC-QTOF-MS/MS of Selected Ions					
MMSR Cluster ID	Retention Time	Correlated PhP Volatiles (*r*)	Mass Spectra Derived by MMSR	Ion Selected for MS/MS	Observed Mass	Calculated Mass [M-H]-	Observed Mass/ Calculated Mass	Elemental Formula	Putative Identity
1	2	3	4	5	6	7	8	9	10
							ppm		
LC1.1	29.51	Eugenol (*r* = 0.8)	503, 457, 293, 504, 505, 113	503	503.1747	503.1770	−4.6	$C_{22}H_{32}O_{13}$	Eugenol-hexose-pentose, FA adduct
					457.1709	457.1715	−1.3	$C_{21}H_{30}O_{11}$	
					293.0868	293.0878	−3.4	$C_{11}H_{18}O_9$	Eugenol-hexose-pentose Hexose + pentose-2H$_2$O
				457	457.1709	457.1715	−1.4	$C_{21}H_{30}O_{11}$	Eugenol hexose-pentose
					293.0880	293.0878	0.7	$C_{11}H_{18}O_9$	Hexose + pentose-2H$_2$O
					163.0766	163.0765	0.9	$C_{10}H_{12}O_2$	Eugenol
LC1.2	19.25	MeSA (*r* = 0.76)	491, 293, 381	491	491.1386	491.1406	−4.1	$C_{20}H_{28}O_{14}$	MeSA hexose-pentose, FA adduct
					445.1347	445.1351	−1.0	$C_{19}H_{26}O_{12}$	
					293.0874	293.0878	−1.4	$C_{11}H_{18}O_9$	MeSA hexose-pentose
					151.0405	151.0401	2.9	$C_8H_8O_3$	Hexose + pentose-2H$_2$O MeSA
LC1.3	16.17	Guaiacol (*r* = 0.78)	463, 417, 293	463	463.1455	463.1457	−0.5	$C_{19}H_{28}O_{13}$	Guaiacol hexose-pentose, FA adduct
					417.1410	417.1402	1.9	$C_{18}H_{26}O_{11}$	
					293.0884	293.0878	2.0	$C_{11}H_{18}O_9$	Guaiacol hexose-pentose Hexose + pentose-2H$_2$O
				417	417.1415	417.1402	3.1	$C_{18}H_{26}O_{11}$	Guaiacol hexose-pentose
					293.0873	293.0878	−1.7	$C_{11}H_{18}O_9$	Hexose + pentose-2H$_2$O
LC2.1	13.58	nd	579	579	579.1925	579.1930	−0.9	$C_{24}H_{36}O_{16}$	Guaiacol dihexose-pentose
					447.1498	447.1506	−1.8	$C_{19}H_{27}O_{12}$	Guaiacol dihexose
					285.0972	285.0978	−2.1	$C_{13}H_{17}O_7$	Guaiacol hexose
LC2.2	17.16	nd	665, 457, 447, 411	665	665.1942	665.1934	1.2	$C_{27}H_{38}O_{19}$	Guaiacol malonyl dihexose-pentose
					579.1927	579.1930	−0.5	$C_{24}H_{36}O_{16}$	Guaiacol dihexose-pentose
					123.0445	123.0452	−5.7	$C_7H_8O_2$	Guaiacol
LC2.3	14.95	nd	607		607.1874	607.1879	−0.8	$C_{25}H_{36}O_{17}$	MeSA dihexose-pentose
					455.1401	455.1395	1.2	$C_{17}H_{28}O_{14}$	Dihexose-pentose
					323.0980	323.0973	2.1	$C_{12}H_{20}O_{10}$	Dihexose
					293.0873	293.0878	−1.7	$C_{11}H_{18}O_9$	Hexose-pentose
LC2.4	18.61	nd	693, 659	693	693.1902	693.1883	2.7	$C_{28}H_{38}O_{20}$	MeSA malonyl dihexose-pentose
					607.1878	607.1879	−0.2	$C_{25}H_{36}O_{17}$	MeSA dihexose-pentose
					151.0411	151.0401	6.8	$C_8H_8O_3$	MeSA
LC2.5	27.25	nd	705 (single)	705	705.2238	705.2247	−1.3	$C_{30}H_{42}O_{19}$	Eugenol malonyl dihexose-pentose
					619.2260	619.2243	2.7	$C_{27}H_{40}O_{16}$	Eugenol dihexose-pentose
					163.0773	163.0765	5.2	$C_{10}H_{12}O_2$	Eugenol
LC2.6	24.85	nd	619	619	619.2236	619.2243	−1.3	$C_{27}H_{40}O_{16}$	Eugenol dihexose-pentose
					323.0978	323.0973	1.5	$C_{12}H_{20}O_{10}$	Dihexose
					455.1401	455.1395	1.2	$C_{17}H_{28}O_{14}$	Dihexose-pentose
					293.0874	293.0878	−1.4	$C_{11}H_{18}O_9$	Hexose-pentose
					163.0761	163.0765	−2.5	$C_{10}H_{12}O_2$	Eugenol

subjected to LC-QTOF-MS/MS fragmentation analyses. First, it was checked whether fragment ions of the volatile PhP aglycones were present in the MS/MS data. The MS/MS fragmentation of the fragment ion m/z 665 eluting at 17.16 min (compound LC2.2; Table I) revealed a fragment ion of $[M - H]^- = 123.0445$, corresponding to the elemental composition of guaiacol (123.0452), and a fragment ion of m/z 579, corresponding to the loss of a malonyl group ($[M - H_2O] = 86$), leaving an elemental composition corresponding to guaiacol bound to a dihexose-pentose sugar moiety. Likewise, the observed LC-MS/MS fragments of the compounds LC2.4 eluting at 18.61 min and LC2.5 eluting at 27.25 min corresponded to MeSA malonyl-dihexose-pentoside and eugenol malonyl-dihexose-pentoside, respectively (Table I). Compound LC2.1 eluting at 13.58 min (parent m/z 579) appeared to be guaiacol dihexose-pentoside. Its MS/MS fragmentation pattern revealed fragments corresponding to dihexose-pentoside (m/z 455), hexose-pentoside (m/z 293), and dihexose (m/z 323), but the loss of the malonyl group was not observed (Table I). The non-malonylated dihexose-pentosides of MeSA and eugenol were also identified (Table I, compounds LC2.3 and LC2.6, respectively). Analysis of MS/MS fragmentation of the other compounds of the LC2 group revealed no relation to the PhP volatiles. Therefore, a potential casual relationship between the presence of

malonyl-dihexose-pentosides and the absence of volatile emission was investigated.

For simplicity, the hexose-pentosides of PhP volatiles found in high-PhP volatile emitters will generally be referred to as "diglycosides," and both the dihexose-pentosides and malonyl-dihexose-pentosides found in low-PhP volatile emitters will generally be referred to as "triglycosides."

The Pool of Glycosidically Bound PhP Volatiles Has the Capacity to Account for the Volatiles Produced upon Fruit Tissue Disruption

It is well known that some tomato volatiles accumulate in fruit tissue during ripening and are stored as nonvolatile sugar conjugates (Buttery et al., 1990; Marlatt et al., 1992; Ortiz-Serrano and Gil, 2007). It has been suggested that the cleavage of such glycosidically bound volatile precursors is mediated through glycosidases liberated or activated upon disruption of cellular compartments when cells become stressed or are damaged (Mizutani et al., 2002). To determine the potential contribution of PhP volatile glycosides to the emission of PhP volatiles upon fruit tissue disruption (blending), we quantified the amounts of glycosidically bound PhP volatiles in tomato fruit by measuring the amounts of PhP volatiles emitted from a crude extract specifically enriched

Figure 2. Amounts (ppm = μL L^{-1} fresh weight) of guaiacol, MeSA, and eugenol emitted from blended fruits of 49 high-PhP volatile (PhP-V) cultivars upon fruit blending (10 min of incubation at 30°C; A) and upon complete viscozyme-mediated in vitro hydrolysis of crude glycoside extracts derived from high- and low-PhP volatile fruits (B). Both PhP volatile diglycosides (C) and triglycosides (D) were completely hydrolyzed after 72 h of viscozyme-mediated hydrolysis. Eug dHP, Eugenol dihexose-pentoside; Eug MdHP, eugenol malonyl-dihexose-pentoside; Gua dHP, guaiacol dihexose-pentoside; Gua MdHP, guaiacol malonyl-dihexose-pentoside; MeSA dHP, MeSA dihexose-pentoside; MeSA MdHP, MeSA malonyl-dihexose-pentoside; SIM, selected ion monitoring.

for glycosides, after treatment with a carbohydrase enzyme preparation possessing a broad spectrum of glycosylhydrolytic activity. To relate these volatile levels to those released upon fruit tissue blending, levels of guaiacol, MeSA, and eugenol emitted from 49 high-PhP volatile fruits of the 94-cultivar collection were quantified using authentic chemical standards. The variation in the levels of guaiacol, MeSA, and eugenol emitted within 10 min after tomato fruit blending is shown in Figure 2A.
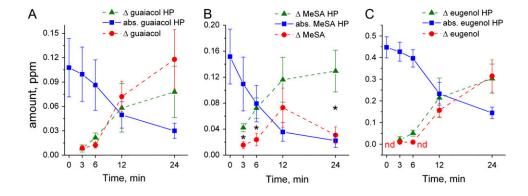
Crude glycosidic extracts were prepared from equal starting amounts of bulked fruit samples of six low- and six high-PhP volatile cultivars and subjected to complete glycoside hydrolysis using Viscozyme L, a crude carbohydrase preparation derived from *Aspergillus* species. Volatiles emitted upon the hydrolysis were analyzed by SPME-GC-MS, and amounts of guaiacol, MeSA, and eugenol were quantified using authentic standards of these compounds, as described in "Materials and Methods." The results show that glycosidic extracts of both high- and low-PhP fruits have a similar capacity to release PhP-derived volatiles upon cleavage by glycosidases (Fig. 2B). Furthermore, the levels of PhP volatiles released from these glycosidic extracts exceeded the amounts of PhP volatiles emitted from high-PhP fruits within 10 min after blending. We calculated that the high-PhP volatile fruit extracts used consisted of 0.096 ± 0.014 μL L^{-1} guaiacol, 0.14 ± 0.008 μL L^{-1} MeSA, and 0.67 ± 0.09 μL L^{-1} eugenol, present as bound glycososides. Low-PhP volatile fruit extracts consisted of 0.066 ± 0.014 μL L^{-1} bound guaiacol, 0.098 ± 0.009 μL L^{-1} bound MeSA, and 0.53 ± 0.034 μL L^{-1} bound eugenol (Fig. 2B). The increase in volatiles released upon glycosidase treatment, both in high- and low-PhP

volatile glycosidic extracts, was accompanied by a complete hydrolysis of the corresponding PhP volatile glycosides (Fig. 2, C and D). These results suggest that the pool of glycosidically bound PhP volatiles has the capacity to account for all the volatiles released upon fruit blending. However, despite the presence of sufficient amounts of glycosidically bound PhP volatiles in low-PhP volatile fruits, these fruits do not release any significant amounts of PhP volatiles upon blending without the need for additional synthesis.

It was not possible to quantify the PhP volatile glycosides directly due to a lack of authentic standards. The viscozyme-mediated hydrolysis, however, enabled us to quantify the amounts of PhP volatile glycosides as amounts of volatiles bound to glycosides by measuring the total amount of volatiles released after complete hydrolysis of the glycosidic extracts.

Cleavage of PhP Volatile Glycosides upon Fruit Tissue Disruption Is Restricted to High-PhP Volatile Fruits

To investigate whether the release of PhP volatiles upon fruit blending was due to endogenous hydrolysis of their corresponding diglycosides, we analyzed the dynamics of PhP volatile emission. Frozen powder of red fruits from six high- and six low-PhP volatile genotypes was incubated for 0, 3, 6, 12, and 24 min at 30°C. At each time point, levels of both volatile and nonvolatile compounds were measured using SPME-GC-MS and LC-QTOF-MS, respectively. In the high-PhP volatile genotypes, emission of all three PhP volatiles increased in time (Fig. 3). For guaiacol and eugenol, emission increased continuously over the 24-min period, while the amount of MeSA released into the head space peaked at 12 min and then decreased

Figure 3. Dynamics of PhP volatile production upon fruit cell disruption. Ground and frozen powder of red fruits from six high-PhP volatile genotypes was incubated for 0, 3, 6, 12, and 24 min at 30°C (which included thawing). At each time point, levels of both volatiles and nonvolatile compounds were measured using SPME-GC-MS and LC-QTOF-MS, respectively. Average patterns (±SD) of six high-PhP volatile genotypes are presented. A, B, and C show emission of guaiacol, MeSA, and eugenol, respectively, and decrease of corresponding hexose-pentosides (HP). Red circles represent amounts of the volatiles emitted at each time point, blue squares represent the calculated absolute (abs.) amount of corresponding hexose-pentosides at each time point, and green triangles represent calculated amounts of corresponding hexose-pentosides cleaved at each time point. Time points at which there is a significant difference (Student's *t* test, $P < 0.05$) between the amount of volatiles emitted (Δ "volatile") and the calculated amount of the corresponding glycosides cleaved (Δ "volatile" HP) are indicated with asterisks. Eugenol was not detected (nd in C) at time points 3 and 6 min. ppm = μL L^{-1}.

(Fig. 3B). Concomitant with the increase in the three volatiles, the levels of their diglycosides decreased. The amounts of guaiacol and eugenol emitted were comparable to the calculated amounts of the corresponding diglycosides cleaved at each of the time points after fruit blending (Fig. 3, A and C). However, emission of MeSA was lower than expected based on the amount of MeSA diglycoside cleaved (Fig. 3B). This might be due to a process acting in parallel to the MeSA release, for example, by conversion or reduction of MeSA before it is emitted into the head space.

Throughout the experiment, no detectable emission of the three PhP volatiles could be observed from fruit material of the low-PhP genotypes (data not shown). In addition, the abundance of all low-PhP volatile triglycoside species remained constant over the 24-min period after fruit blending (Fig. 4), indicating that their cleavage did not occur. This is in contrast, as described above, to the case of high-PhP volatile cultivars, where this incubation period was clearly sufficient to release enough PhP volatiles from their corresponding diglycosides to account for the total amount of volatiles produced (Fig. 3). Low-PhP volatile fruits, therefore, lack the capacity to emit guaiacol, MeSA, and eugenol from their corresponding triglycosides upon fruit tissue disruption.

PhP Volatile Glycosides Identified in Low-PhP Volatile Fruits Are Resistant to Endogenous Hydrolysis upon Fruit Tissue Disruption

The observations above may be due either to differences in glycosidase activity of high- and low-PhP volatile fruit matrix or to differences in susceptibility of the high- and low-PhP volatile glycoside species to endogenous glycosidases. To investigate this, low- and high-PhP volatile fruit materials (bulks of fruits of the six low-PhP volatile and the six high-PhP volatile cultivars used for experiments described above) were spiked with glycosidic extracts containing different PhP glycosides in a reciprocal way. First, we studied whether the low-PhP volatile fruit matrix has the capacity to hydrolyze PhP volatile diglycosides similar to the high-PhP volatile fruits they were derived from. For this, a crude glycosidic extract derived from high-PhP volatile fruits and previously used for the quantitative analysis of bound PhP volatiles (Fig. 2B), containing diglycosides of guaiacol, MeSA, and eugenol, was added to (1) blended low-PhP volatile fruits and (2) blended high-PhP volatile fruits as a control. LC-MS analysis of spiked and nonspiked tomato matrix revealed that the following amounts of PhP volatile diglycosides were spiked in: 0.40 ± 0.023 μL L^{-1} guaiacol, 0.63 ± 0.018 μL L^{-1} MeSA, and 4.28 ± 0.26 μL L^{-1} eugenol. The spiked fruit samples were incubated for 10 min at 30°C as described before. Spiking of high-PhP volatile fruits with a high-PhP volatile glycosidic extract containing PhP volatile diglycosides resulted in significant increases in the emission of the PhP volatiles guaiacol (Δemission = 0.106 ± 0.01
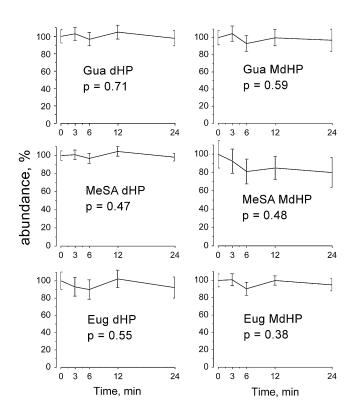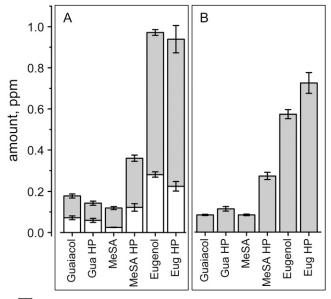

Figure 4. Dynamics of PhP volatile glycosides in low-PhP volatile fruits upon fruit cell disruption. Ground and frozen powder of red fruits from six low-PhP volatile genotypes was incubated for 0, 3, 6, 12, and 24 min at 30°C (which included thawing). At each time point, levels of the PhP volatile glycosides guaiacol dihexose-pentoside (Gua dHP) and malonyl-dihexose-pentoside (Gua MdHP), MeSA dihexose-pentoside (MeSA dHP) and malonyl-dihexose-pentoside (MeSA MdHP), and eugenol dihexose-pentoside (Eug dHP) and malonyl-dihexose-pentoside (Eug MdHP) were measured using LC-QTOF-MS. Abundances are represented as percentage of abundance of each of the compounds at time point 0 min. Gua dHP and Gua MdHP consist of 0.066 ± 0.014 μL L^{-1} bound guaiacol, MeSA dHP and MeSA MdHP consist of 0.098 ± 0.009 μL L^{-1} bound MeSA, and Eug dHP and Eug MdHP consist of 0.53 ± 0.034 μL L^{-1} bound eugenol at starting time point 0. Average patterns ($\pm$SD) of six low-PhP volatile genotypes are presented. Multiple ANOVAs were performed to estimate the difference between time points of each of the compounds, and corresponding P values are presented.

μL L^{-1}; $P < 0.01$ [significance of difference compared with the nonspiked control]), MeSA (Δemission = 0.094 ± 0.007 μL L^{-1}; $P < 0.001$), and eugenol (Δemission = 0.69 ± 0.014 μL L^{-1}; $P < 0.001$) compared with the amounts of these volatiles emitted from nonspiked high-PhP volatile fruit material (Fig. 5A). The amounts of diglycosides decreased accordingly, except for MeSA, which was emitted at a lower amount than was anticipated based on the hydrolysis of the corresponding diglycoside. A comparable increase in the emission of PhP volatiles was found when low-PhP volatile fruit matrix was spiked with a high-PhP volatile glycosidic extract (Fig. 5B). These results indicate that low-PhP volatile fruits have a glycosylhy-

Figure 5. Spiking of blended tomato fruit with high-PhP volatile (PhP-V) glycosidic extracts. High-PhP (A) and low-PhP (B) volatile fruit matrix was spiked with a crude glycoside extract obtained from high-PhP volatile fruits and consisting of PhP volatile diglycosides (hexose-pentosides; HP). Emission of volatiles was measured using GC-MS, and reduction of PhP volatile diglycosides was measured using LC-QTOF-MS and expressed as μL L^{-1} volatiles emitted, as described in "Materials and Methods." White bars represent nonspiked control samples, and gray bars represent additional amount of volatiles emitted or glycosides (hexose-pentosides) hydrolyzed in spiked samples. ppm = μL L^{-1}.
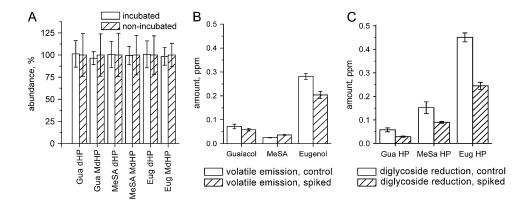
drolytic activity similar to high-PhP volatile fruits and suggest that the difference in PhP volatile emission observed between fruits of the two groups of tomatoes is due to resistance of low-PhP volatile glycosides to endogenous hydrolysis rather than to differences in glycosidase activity.

To study this hypothesis, the high-PhP volatile fruit matrix was spiked with a crude low-PhP glycosidic extract containing triglycosides. Based on the proportions of diglycoside and triglycoside content in high- and low-PhP volatile glycosidic extracts, respectively (Fig. 2B), we calculated that the following additional amounts of PhP volatile triglycosides were present in spiked samples: 0.28 ± 0.05 μL L^{-1} bound guaiacol, 0.44 ± 0.04 μL L^{-1} bound MeSA, and 3.38 ± 0.23 μL L^{-1} bound eugenol. None of the spiked guaiacol, MeSA, and eugenol triglycosides were cleaved (Fig. 6A), confirming that these triglycosidic forms are resistant to hydrolysis by the endogenous glycosidases in both low- and high-PhP volatile fruits. Indeed, spiking with low-PhP volatile glycosides did not lead to any significant increase in the emission of guaiacol and eugenol compared with the nonspiked control (Fig. 6B), and the levels of these compounds

could well be explained by the amount of the corresponding diglycosides cleaved (Fig. 6C). However, rather than increased, emission of both guaiacol and eugenol tended to be decreased relative to the nonspiked control (Fig. 6B). For eugenol, this decrease appeared to be significant ($P < 0.001$). This was consistent with a decrease in hydrolysis of the corresponding diglycosides (Fig. 6C). The observed decrease in diglycoside hydrolysis/volatile emission suggests that the activity of the endogenous glycosyl hydrolase is inhibited by the crude low-PhP glycosidic extract. One could speculate that the excess of PhP triglycosides added inhibits the glycosyl hydrolase activity, for example, by competing with the endogenous diglycosides for binding to the active site of the glycosyl hydrolase enzyme.

Also, the cleavage of MeSA diglycoside was inhibited by the low-PhP glycosidic extract, but the amounts cleaved could well account for the amount of MeSA released (Fig. 6, B and C). Surprisingly, however, the emission of MeSA did not follow the pattern of the diglycoside cleavage, since it slightly increased in spiked samples, rather than decreased (Fig. 6B). This apparent discrepancy is most likely due to an effect of the crude low-PhP glycosidic extract on processes that may be acting in parallel to the MeSA release, as observed in the time-course experiments (Fig. 3B).

The PhP Volatile Emission Contrast Develops during Fruit Ripening

Evidently, the difference in PhP volatile emission between ripe fruits from low- and high-PhP volatile tomato cultivars is related to the difference in their glycosylation patterns. To investigate whether fruit development plays a role in establishing the observed difference in PhP volatile glycosylation, we studied the dynamics of both PhP volatile emission and glycoside accumulation during normal fruit ripening. Fruits of three low- and three high-PhP volatile genotypes were harvested at mature green, breaker, turning, and red-ripe stages. The emission of PhP volatiles after blending was analyzed by SPME-GC-MS, and the amounts of the corresponding glycosides in the intact fruit were determined by LC-QTOF-MS. In fruits of high-PhP volatile genotypes, the levels of the PhP volatiles guaiacol and MeSA emitted at mature green, breaker, and turning stages were found to be similar to the levels observed in red-ripe fruits of these genotypes (Fig. 7, A and B). The emission of eugenol from mature green fruits was low but increased markedly upon fruit maturation (Fig. 7C). The abundance of all three PhP volatile diglycosides in intact fruits showed patterns similar to those of the volatile aglycones (Fig. 7, D–F). Mature green fruits of the low-PhP volatile cultivars emitted amounts of guaiacol, MeSA, and eugenol that were comparable with those observed in green fruits of high-PhP volatile genotypes (Fig. 7, A–C). This was also observed for the corresponding diglycosides, except for

Figure 6. Spiking of high-PhP volatile fruits blended with glycoside extract obtained from low-PhP volatile fruits containing triglycosides and malonyl triglycosides of guaiacol, MeSA, and eugenol. A, Relative amounts of PhP volatile triglycosides in blended high-PhP volatile fruits spiked with a triglycoside extract, measured before and after incubation for 10 min at 30°C. LC-MS signal intensities of malonylated and nonmalonylated triglycosides of each of the volatiles were expressed as percentage of the levels in the nonincubated sample. The following calculated amounts of bound PhP volatiles (as triglycosides and malonyl triglycosides) were spiked: $0.28 \pm 0.05~\mu\text{L L}^{-1}$ guaiacol, $0.44 \pm 0.04~\mu\text{L L}^{-1}$ MeSA, and $3.38 \pm 0.23~\mu\text{L L}^{-1}$ eugenol. Eug dHP, Eugenol dihexose-pentoside; Eug MdHP, eugenol malonyl-dihexose-pentoside; Gua dHP, guaiacol dihexose-pentoside; Gua MdHP, guaiacol malonyl-dihexose-pentoside; MeSA dHP, MeSA dihexose-pentoside; MeSA MdHP, MeSA malonyl-dihexose-pentoside. B, Amounts of PhP volatiles emitted from nonspiked high-PhP volatile fruits blended and incubated for 10 min at 30°C (control, white bars) and from blended high-PhP volatile fruits spiked with a glycoside extract containing triglycoside and malonyl trihexose-pentosides of guaiacol, MeSA, and eugenol (striped bars). C, Reduction of PhP volatile diglycosides after 10 min of incubation at 30°C of blended high-PhP volatile fruits (white bars) or in blended high-PhP fruits spiked with a triglycoside extract (striped bars). Reduction of PhP volatile diglycosides was measured using LC-QTOF-MS and expressed as $\mu\text{L L}^{-1}$ volatiles emitted, as described in "Materials and Methods." ppm = $\mu\text{L L}^{-1}$.

eugenol diglycoside, which could not be detected in low-PhP volatile fruits at any of the ripening stages (Fig. 7, D–F). During maturation of low-PhP volatile fruits, levels of both the PhP volatiles and the corresponding diglycosides declined to barely detectable levels at turning and red-ripe stages. However, this decline was accompanied by an increase in the levels of all PhP volatile triglycosides (Fig. 7, G–I). These results clearly show that, in fruits of high-PhP volatile cultivars, PhP volatiles can be emitted at all stages of ripening. However, low-PhP volatile lines only have this capacity at the mature green stage. This suggests that a developmentally regulated program, switched either on or off at the breaker stage, determines the emission of PhP volatiles in fruits of high- versus low-PhP volatile cultivars by modifying the chemical structure of their nonvolatile glycosidic precursors. The conversion from a diglycoside into a (malonyl)triglycoside likely prevents the glycosidic bonding being cleaved by endogenous enzymes. Consequently, aglycone release upon tissue disruption is prevented, thus leading to the low-PhP volatile phenotype in red fruit (Fig. 8). This suggests a novel concept for the regulation of PhP volatile production, not by activating or deactivating the volatile biosynthetic pathway but by changing the glycoconjugate structure of the volatile precursors in question, thereby making them unavailable to subsequent enzymatic hydrolysis upon decompartmentalization.

DISCUSSION

Emission of PhP Volatiles from Tomato Fruit upon Tissue Disruption Is Due to Cleavage of the Corresponding Hexose-Pentosides

We have previously shown that polyphenol compounds in general play a significant role in determining the phenotypic and biochemical differences between tomato tissues and genotypes (Bovy et al., 2007, 2010; Moco et al., 2007; Butelli et al., 2008; Schijlen et al., 2008). The production of PhP volatiles, such as MeSA, guaiacol, and eugenol, was also found to be one of the most important determinants of the metabolic variation in a set of 94 tomato cultivars chosen to represent the current commercial tomato germplasm. The ability to emit these volatiles upon fruit tissue disruption divided the genotype set into two groups, irrespective of their physical phenotype (Tikunov et al., 2005).

Analysis of complex metabolomics data reveal that correlating compounds are often biochemically related or they can be linked as precursor-product in a biochemical pathway (Ursem et al., 2008; Gavai et al., 2009). In this study, we aimed to unravel the biochemical mechanisms underlying the observed difference in PhP volatile emission by searching for causal relationships between volatiles and their potential biochemical precursors, nonvolatile compounds. Therefore, red-ripe fruits of 94 tomato cultivars were profiled using SPME-GC-MS to detect volatiles and
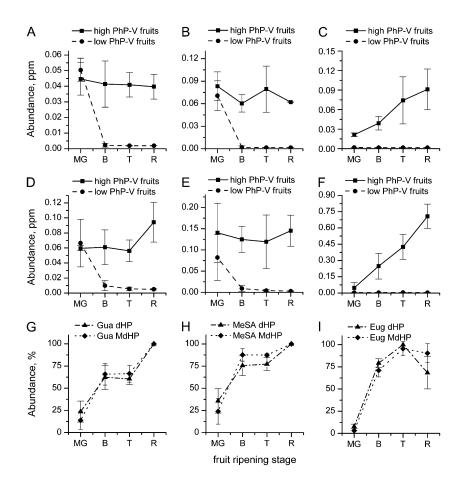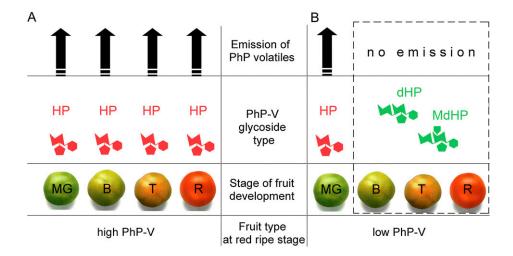
Figure 7. Analysis of the PhP volatiles and their respective glycosides during tomato fruit development in high- and low-PhP volatile (PhP-V) genotypes. Frozen powder of three high- and three low-PhP volatile genotypes was incubated for 10 min at 30°C, and levels of volatiles released (after 10 min of incubation) and of their corresponding glycosides (in intact fruit, prior to incubation) were measured by GC-MS and LC-MS, respectively. Results show average patterns of high- and low-PhP volatile genotypes. A to C, PhP volatiles guaiacol, MeSA, and eugenol, respectively. D to F, PhP volatile diglycosides (hexose-pentosides) of guaiacol, MeSA, and eugenol, respectively. G to I, PhP volatile triglycosides (dihexose-pentosides [dHP]) and malonyl triglycosides (malonyl-dihexose-pentosides [MdHP]) of guaiacol (Gua), MeSA, and eugenol (Eug), respectively, in low-PhP lines. (High-PhP lines showed no/negligible levels of triglycosides, so those results are not presented.) Abundance of triglycosides and malonyl triglycosides is presented as a percentage of the maximum intensity of a compound's parent ion detected by LC-MS. At red-ripe stage, both triglycosides and malonyl triglycosides represent 0.066 ± 0.014 μL L^{-1} bound guaiacol, 0.098 ± 0.009 μL L^{-1} bound MeSA, and 0.53 ± 0.034 μL L^{-1} bound eugenol. MG, B, T, and R represent the tomato fruit developmental stages mature green, breaker, turning, and red ripe, respectively. ppm = μL L^{-1}.

LC-QTOF-MS to detect semipolar, nonvolatile metabolites. Data fusion strategies using GC-MS and LC-MS data sets, followed by multivariate analysis, revealed a genotype structure that was mostly determined by the PhP volatiles and a number of nonvolatile metabolites. Those nonvolatile metabolites that correlated positively to the PhP volatiles were putatively identified as being the diglycosides of these volatiles, consisting of a hexose-pentose moiety as determined by LC-MS and LC-MS/MS accurate mass fragmentation patterns. The analytical tools used, however, do not allow for discrimination between different pentose and hexose sugar isomers. Several hexose-pentose combinations, ubiquitous in nature, can potentially be attached to these volatile aglycones, producing different types of diglycosides, such as β-L-arabinofuranosyl-β-D-glucopyranosid, β-D-apiofuranosyl-β-D-glucopyranoside (vicianoside), and β-D-xylopyranoyl-β-D-glucopyranoside (primeveroside; Crouzet and Chassagne, 1999).

Many volatile compounds are detectable as glycoconjugates in tomato fruit (Buttery et al., 1990; Marlatt et al., 1992; Ortiz-Serrano and Gil, 2007). Emission of the three PhP volatiles studied here has been observed upon enzymatic or acid hydrolysis of tomato fruit glycosidic extracts (Marlatt et al., 1992; Ortiz-Serrano and Gil, 2007). In vivo, volatile compounds can be liberated from their glycosidically bound forms (e.g.

upon plant cell disruption during herbivore attack, fruit processing, or consumption). Cell disruption leads to mixing of subcellular compartments; thus, volatile glycosides become exposed to endogenous or exogenous cleavage enzymes, such as glycosyl hydrolases (glycosidases). Our results suggest that the quick and intense emission of PhP volatiles occurring upon fruit tissue disruption (blending) can be explained by cleavage of the corresponding diglycosides by endogenous glycosidase(s), since (1) the tomato fruit tissue disruption time-course experiment (Fig. 3) showed that the increase of PhP volatile emission was accompanied by a quantitatively comparable reduction of the corresponding diglycosides; (2) the in vitro hydrolysis of crude tomato fruit glycosides mediated by a carbohydrase preparation showed that the pool of glycosidically bound PhP volatiles has the capacity to account for the volatiles produced upon tissue grinding; and (3) spiking blended tomato fruit matrix with a crude glycosidic extract derived from high-PhP volatile fruit material, containing PhP volatile diglycosides, resulted in enhanced emission of PhP volatiles not only when spiked in the high-PhP volatile fruit matrix but also upon spiking into the low-PhP volatile fruit matrix. The latter result indicates that both high- and low-PhP volatile tomato fruits have a similar capacity to cleave PhP volatile diglycosides upon

Figure 8. Model of PhP volatile (PhP-V) emission in low- and high-PhP volatile genotypes through a ripening-dependent diversification of PhP volatile glycoconjugate patterns. PhP volatile hexose-pentosides (HP) are present at mature green (MG), breaker (B), turning (T), and red-ripe (R) stages of high-PhP volatile genotypes (A) as well as at the mature green stage of low-PhP volatile genotypes (B). These diglycosides can be cleaved upon fruit cell disruption, leading to emission of the corresponding volatile aglycones. Emission of PhP volatiles is arrested in fruits of low-PhP volatile genotypes from breaker stage onward due to conversion of PhP volatile hexose-pentosides into PhP volatile dihexose-pentosides (dHP) and malonyl-dihexose-pentosides (MdHP), which are resistant to the endogenous tomato glycosylhydrolitic activity induced upon fruit tissue disruption.

tissue disruption but that volatile emission is determined by the presence of these specific volatile diglycosides in the tomato fruit.

Interestingly, in the tomato fruit blending time-series experiment, the amount of MeSA emitted into the head space increased in time until a maximum emission was reached at approximately 10 min of incubation and decreased again at longer incubation times. At the same time, the amount of the corresponding hexose-pentoside was nevertheless continuously reduced over the entire 24-min period. We hypothesize that this decrease is due to a process that acts in parallel to the release of methyl salicylate and causes endogenous loss of MeSA (e.g. through its conversion into the nonvolatile salicylic acid). This process has already been described for MeSA in relation to its airborne signaling ability (Shulaev et al., 1997). These authors demonstrated that MeSA could be transmitted to neighboring plants and subsequently induce their defensive mechanisms by converting MeSA into salicylic acid. The enzyme SABP2 (for salicylic acid-binding protein) mediating the conversion of MeSA into salicylic acid has been identified (Forouhar et al., 2005). Thus, MeSA acts as mobile signal molecule in systemic acquired resistance (Park et al., 2007). If this well-known process also takes place in tomato fruit, our experiments demonstrate the existence of a mechanism to initiate such communication through a quick release of considerable amounts of MeSA and the other two PhP volatiles, guaiacol and eugenol, by cleavage of their corresponding diglycosides upon tissue damage/disruption. This process may be of particular importance in leaves, where we could detect all three PhP volatile

hexose-pentosides in both high- and low-PhP volatile genotypes (data not shown).

PhP Volatile Emission Is Arrested in Low-PhP Volatile Fruits Due to a Ripening-Induced Modification of the Glycosylation Pattern

Emission of PhP volatiles upon tissue disruption, by cleavage of the corresponding diglycosides, was observed in fruits of only a portion of the cultivars tested. We hypothesized that in fruits that did not emit PhP volatiles, these compounds were present in a different noncleavable form. Indeed, when fusing GC-MS and LC-MS data sets, we identified nonvolatile metabolites that accumulated in low-PhP volatile fruits and that were inversely correlated to the presence of PhP volatiles and their nonvolatile diglycoside precursors. Later, GC-MS and LC-MS analysis of crude glycoside extracts hydrolyzed in vitro using a fungal crude carbohydrase preparation revealed that the amount of PhP volatiles emitted from crude glycosides extracted from low-PhP volatile fruits was comparable to the amount of these volatiles emitted from high-PhP volatile glycoside extracts (Fig. 2B). These observations led to the hypothesis that in low-PhP volatile fruits, PhP volatiles were present but in a different conjugated form. Essentially, in low-PhP fruits, conjugation goes a step further during ripening. The new conjugated forms could be cleaved with the carbohydrase preparation in vitro to emit PhP volatiles but not by endogenous carbohydrases naturally present in tomato fruits. Using LC-MS/MS analyses, we found that in the low-PhP volatile fruits, MeSA, guaiacol, and eugenol are

present as various glycoside species different from the hexose-pentosides present in high-PhP volatile fruits. Analysis of MS/MS spectra of these glycosides revealed two major sugar moieties conjugated to guaiacol, MeSA, and eugenol: (1) a dihexose-pentose moiety, and (2) a malonyl dihexose-pentose moiety. Triglycosides of volatiles consisting of different sugar combinations have been reported in plants before (Herderich et al., 1992; Bilia et al., 1994; Kijima et al., 1997). Also, malonylation of sugar moieties is a common feature in several plants (Withopf et al., 1997; Kazuma et al., 2003; D'Auria et al., 2007; Kogawa et al., 2007). To our knowledge, however, malonylated triglycosides of volatile compounds have not been described in plants to date. Malonylation of secondary metabolite glycosides might play a role in enhancing metabolite solubility, resistance to glycosidase-driven cleavage, and differential targeting of organic compounds to either the vacuole or the cell wall (Day and Saunders, 2004; Dhaubhadel et al., 2008). Our results, showing that neither dihexose-pentosides of PhP volatiles nor their malonylated forms could be cleaved by endogenous glycosylhydrolases induced upon disruption of both low- and high-PhP volatile fruits, indicate that the addition of the second hexose rather than the malonylation is the primary factor determining the resistance of the low-PhP volatile triglycoside species to endogenous hydrolysis. The additional malonylation might serve other functional purposes.

Unripe mature green fruits of both low- and high-PhP volatile emitters (at red-ripe stage) revealed the presence of comparable amounts of PhP volatile diglycosides. As a result, both types of fruit did not reveal a significant difference in PhP volatile emission at this ripening stage. Along with the results of the in vitro enzymatic hydrolysis of red-ripe fruit glycosidic extracts, these results suggest that the biosynthetic pathways leading to the production of the three PhP volatiles are equally active in both types of fruit and have the capacity to produce comparable amounts of these volatiles throughout fruit ripening. The difference in emission of PhP volatiles upon fruit blending develops as fruit ripening progresses and results from the ripening-dependent additional modification of the glycosylation patterns of these volatiles. In low-PhP volatile fruits, the cleavable PhP volatile diglycoside species are converted into noncleavable triglycoside species from breaker stage onward. The addition of the second hexose onto the first hexose of the diglycoside, which is obvious from the MS/MS fragmentation (Table I) where dihexose fragments could be found, prevents hydrolysis of the resulting triglycosides upon fruit blending (Fig. 8).

At present, we can only speculate on which genes and/or enzymes are involved in the synthesis of the PhP volatile triglycosides. Furthermore, we also have no clear view as to their genetic origin or to how their distribution relates to parentage. Likely, the enzymes belong to two classes: (1) glycosyl transferases, which transfer a nucleotide diphosphate-activated sugar group to an aglycone or an already existing sugar moiety; and (2) malonyl transferases, transferring a malonyl group from malonyl-CoA to a sugar moiety. Approximately 15 malonyltransferases have been described in the plant kingdom to date (D'Auria, 2006; Suzuki et al., 2007; Unno et al., 2007). More than 100 glycosyl transferases with a glycosylation activity for small molecules have been described in Arabidopsis (Bowles et al., 2005). Functional characteristics and substrate specificities of many of these genes are not completely known. Preliminary results of our own gene expression experiments revealed approximately 100 glycosyl transferase genes expressed in tomato fruit (data not shown). We are currently employing various strategies (genetic, expression, and functional gene analyses) to find those glycosyl transferase genes involved in the PhP volatile glycoside modification. In summary, we showed that, in tomato fruit, emission of the PhP volatiles guaiacol, MeSA, and eugenol appear to be regulated by means of a developmentally programmed modification of their glycosylated precursors. Tomato fruits have a large reserve of important flavor volatiles stored as glycosides (Buttery et al., 1990; Marlatt et al., 1992; Ortiz-Serrano and Gil, 2007). This principle influencing the emission of flavor volatiles through their glycoconjugate modification could pave the way for new strategies to control fruit quality characteristics such as flavor and taste. Besides fruit quality aspects, this biochemical process may also play an important role in plant-environment interactions, including the response to biotic stresses. At this point, it is not completely clear how this mechanism has evolved. It could have appeared as a by-product of extensive tomato breeding activities and now can be considered as a potentially beneficial trait. On the other hand, considering that fruit flavor is an important characteristic for natural seed-dispersing organisms (Goff and Klee, 2006; Schwab et al., 2008), one can assume that this mechanism could have already evolved in wild tomato (Solanum spp.) germplasm. Indeed, we have preliminary data suggesting that there is variation for this trait in wild tomato germplasm (data not shown). Nevertheless, this question will require further investigation. A combination of fusion of data derived from a modern multiinstrumental metabolic profiling platform and a classical quantitative analysis of biochemical processes appears to be a powerful approach to elucidate the biochemical principle underlying PhP volatile emission in tomato fruit. In addition, many other volatile-nonvolatile metabolite interactions could be observed. Our current activities are aimed at unraveling the functional significance of a broader range of these interactions.

MATERIALS AND METHODS

Plant Material

Seeds from 94 tomato (*Solanum lycopersicum*) cultivars were obtained from six different tomato seed companies, each having its own breeding program.

As such, the cultivars should represent a considerable collection of genetic and therefore phenotypic variation, not just between tomato types (cherry, round, and beef) but also within the individual genotypes of each fruit type. This study was initially performed "blind," and the only information received from the company breeders concerned fruit type. No information was supplied on their genetic backgrounds. For fruit type classification, breeders generally use a combination of (1) fruit diameter and (2) number of locules in the fruit (fl). For the latter, the criteria were as follows: cherry type, fl = 2; round, fl = 3; beef, fl ≥ 4. Two independent experiments were performed over two seasons: one in 2003 and one in 2004. A study of the volatile compounds from ripe fruits of plants, specifically from the 2003 experiment, has been described before (Tikunov et al., 2005). This study was performed on the second experiment carried out in 2004. As in 2003, all cultivars were grown in the summer under greenhouse conditions at a single location in Wageningen, The Netherlands. Nine plants, randomly distributed over three adjacent greenhouse compartments, were grown for each cultivar, giving a total of approximately 850 individuals. Pink-staged tomato fruits were picked from all plants on two consecutive days. To mimic the conditions "from farm to fork," fruits were then stored for 1 week at 15°C followed by 1 d at 20°C prior to sampling and freezing in liquid nitrogen. During this 8-d period, the fruits continued to ripen slowly and, at the moment of sampling, were fully red-ripe, resembling the situation at the time of consumption. In addition, fruits of each of the 94 cultivars were collected at three developmental stages: mature green, breaker, and turning. These stages were judged according to a standardized fruit color scheme provided by The Greenery (Valstar Holland). To make a representative fruit sample, for each cultivar and at each of the four ripening stages, a number of identical red-ripe fruits was pooled; 12 for round and beef tomatoes and 18 for cherry tomatoes. The fruit material was immediately frozen in liquid nitrogen, ground in an analytical electric grinder, and stored at −80°C until analysis.

SPME-GC-MS Profiling of Tomato Fruit Volatile Organic Compounds

The profiling of volatile metabolites was performed using a head space SPME-GC-MS method (Tikunov et al., 2005, 2007). Frozen fruit powder (1 g fresh weight) was weighed into a 5-mL screw-cap vial, closed, and incubated at 30°C for 10 min. An aqueous EDTA-NaOH solution was prepared by adjusting 100 mM EDTA to pH 7.5 with NaOH. Then, 1 mL of the EDTA-NaOH solution was added to the sample to give a final EDTA concentration of 50 mM. Solid $CaCl_2$ was then immediately added to give a final concentration of 5 M. The closed vials were then sonicated for 5 min. A 1-mL aliquot of the pulp was transferred into a 10-mL crimp cap vial (Waters), capped, and used for SPME-GC-MS analysis.

Volatiles were automatically extracted from the vial head space and injected into the GC-MS apparatus via a Combi PAL autosampler (CTC Analytics). Head space volatiles were extracted by exposing a 65-μm PDMS-DVB SPME fiber (Supelco) to the vial head space for 20 min under continuous agitation and heating at 50°C. The fiber was desorbed in a GC 8000 (Fisons Instruments) injection port for 1 min at 250°C. Chromatography was performed on an HP-5 (50 m × 0.32 mm × 1.05 μm) column with helium as carrier gas (37 kPa). The GC interface and MS source temperatures were 260°C and 250°C, respectively. The GC temperature program began at 45°C (2 min), was then raised to 250°C at a rate of 5°C min^{-1}, and finally was held at 250°C for 5 min. The total run time including oven cooling was 60 min. Mass spectra in the 35 to 400 m/z range were recorded by an MD800 electron-impact MS apparatus (Fisons Instruments) at a scanning speed of 2.8 scans s^{-1} and an ionization energy of 70 eV. The chromatography and spectral data were evaluated using Xcalibur software (http://www.thermo.com).

LC-QTOF-MS and MS/MS Analyses of Semipolar Tomato Fruit Compounds

The extraction and the LC-QTOF-MS analysis of semipolar compounds were performed according to the protocol described by Moco et al. (2006); 0.5 g of frozen tomato fruit powder (fresh weight) of each of the 94 cultivars was extracted with 1.5 mL of formic acid:methanol (1:1,000, v/v) solution. The extracts were sonicated for 15 min and filtered through a 0.2-μm inorganic membrane filter (Anotop 10; Whatman).

An LC-QTOF-MS platform was used for the profiling of extracts. This platform consisted of a Waters Alliance 2795 HT HPLC system equipped with a Luna C18(2) precolumn (2.0 × 4 mm) and an analytical column (2.0 × 150 mm, 100 Å, particle size 3 μm; Phenomenex) connected to an Ultima V4.00.00 QTOF mass spectrometer (Waters, MS Technologies). Degassed solutions of formic acid:ultrapure water (1:1,000, v/v; eluent A) and formic acid:acetonitrile (1:1,000, v/v; eluent B) were pumped into the HPLC system at 190 μL min^{-1}, and the gradient was linearly increased from 5% to 35% eluent B over a 45-min period, followed by 15 min of washing and equilibration of the column. The column, sample, and room temperatures were kept at 40°C, 20°C, and 20°C, respectively.

Ionization was performed using an electrospray ionization source, and masses were detected in negative mode. A collision energy of 10 eV was used for full-scan LC-MS in the range of m/z 100 to 1,500. For LC-MS/MS, increasing collision energies of 10, 15, 25, 35, and 50 eV were applied. Leu enkephalin, [M − H]$^-$ = 554.2620, was used for online mass calibration (lock mass).

Preparation of Tomato Fruit Extracts Enriched with Crude Glycosides

Two bulked tomato fruit samples, high-PhP volatile and low-PhP volatile, were prepared by mixing equal amounts of six high-PhP volatile and six low-PhP volatile genotypes, respectively. Methanolic extracts were prepared by the extraction of 40 g fresh weight of each of the bulks in 120 mL of 100% methanol with 1 h of agitation at room temperature. The methanol was then removed from the supernatant in a vacuum rotary evaporator at 40°C, and the glycoside residue was redissolved in 50 mL of pure water. The extract was passed through a glass column (35 × 1 cm i.d.) packed with up to 20 cm of Amberlite XAD-2 resin (Supelco). The flow rate used was 2 mL min^{-1}. The column was then rinsed with 50 mL of water, followed by 50 mL of hexane. Bound compounds were then eluted from the column using 50 mL of methanol, which was then evaporated under vacuum at 40°C.

Quantitative Analysis of Glycosidically Bound PhP Volatiles

A lack of authentic chemical standards did not allow direct quantification of PhP volatile glycosides identified in this study. Authentic chemical standards of guaiacol, MeSA, and eugenol are available (Sigma-Aldrich). Thus, the amounts of PhP volatile glycosides, measured as LC-MS detector response of a parent molecular ion, were expressed as amounts of corresponding volatiles (in μL L^{-1}) released upon their complete hydrolysis. For this, dilution series of crude glycosides extracted from both low- and high-PhP volatile fruits were prepared and subjected to enzymatic hydrolysis and amounts of glycosides present and volatiles released were measured by LC-QTOF-MS and SPME-GC-MS, respectively. First, aliquots of a glycosidic extract each corresponding to 16 g fresh weight of original fruit tissue material of low- and high-PhP volatile fruits were redissolved in 1.5 mL of phosphate-citrate buffer (0.2 M, pH 5.4). The solution obtained was divided into two series of five aliquots of 50, 100, 150, 200, and 250 μL. The first aliquot series was used to estimate original amounts of PhP volatile glycosides present. For this, each of the aliquots was adjusted to 1 mL with phosphate-citrate buffer and 3 mL of methanol was added. The solutions obtained were analyzed by LC-QTOF-MS. One of the two aliquot series was placed in 1.5-mL screw-cap vials, 200 μL of Viscozyme L (Sigma-Aldrich; a carbohydrase preparation derived from *Aspergillus* species) was added to each of the aliquots as a hydrolytic agent, and the total volume of each of the samples was adjusted to 1 mL with the phosphate-citrate buffer. Vials were closed and incubated at 40°C for 72 h. After the incubation, 0.5 mL of each sample was extracted with 1.5 mL of methanol and subjected to LC-QTOF-MS analysis as described above to ensure complete hydrolysis of PhP volatile diglycosides. The remaining 0.5 mL of each of the hydrolyzed samples was mixed with 0.5 mL of NaOH-EDTA mixture (100 mM, pH 7.5) and solid $CaCl_2$ (5 M final concentration) in a 10-mL head space vial. These samples were subjected to SPME-GC-MS analysis of volatile compounds produced upon glycoside hydrolysis. Amounts of guaiacol, MeSA, and eugenol emitted after hydrolysis of glycosides were quantified using calibration curves. For this purpose, different amounts of authentic standards of these volatiles were diluted in medium that was identical to the medium used for the enzymatic hydrolysis and analyzed by SPME-GC-MS. The following concentration ranges of volatiles were used: 0.1 to 0.5 μL L^{-1} guaiacol and MeSA and 0.05 to 0.25 μL L^{-1} eugenol. The calculated amounts of bound volatiles in crude glycosidic extracts, determined through their release after viscozyme treatment, are expressed as μL L^{-1} present in the original high- and low-PhP tomato fruits (Fig. 2B).

As shown in "Results," in high-PhP volatile fruits guaiacol, MeSA, and eugenol exist as a single major glycoconjugated form: diglycosides (hexose-pentosides). Thus, the amounts of PhP volatile diglycosides could be expressed as μL L^{-1} using linear equations derived by fitting the diglycoside LC-MS responses of the nonhydrolyzed glycoside aliquot series to quantitative data of volatiles released upon their complete hydrolysis achieved in 72 h: $y = a + b*x$, where y is a diglycoside MS detector response, x is the amount of a corresponding volatile released upon the complete diglycoside hydrolysis in μL L^{-1}, a is an intercept set at 0, and b is a coefficient that is equal to $0.00431 \pm 3e\text{-}4$ for guaiacol, $0.00285 \pm 5e\text{-}5$ for MeSA, and $0.00329 \pm 2.7e\text{-}4$ for eugenol. These equations were used to quantify amounts of diglycosides in all experiments of this study.

Individual quantification of the PhP volatile triglycosides present in the low-PhP volatile fruits was not possible, since they exist in two major forms, dihexose-pentosides and malonyl-dihexose-pentosides, which can have different ionization efficiencies. Therefore, the amounts of the PhP volatile triglycosides in the fruit tissue disruption series, the spiking experiments, and the analysis of fruit ripening stages were expressed relative (%) to their levels in intact red ripe fruits. The total amount of bound volatiles that both triglycoside forms account for could be calculated based on the viscozyme-mediated hydrolysis, as described above.

Analysis of PhP Volatile Emission and PhP Volatile Glycoside Hydrolysis upon Tomato Fruit Disruption

Aliquots of 1 g fresh weight of red ripe fruit material of each of the cultivars selected for the experiment were incubated in duplicate in closed 5-mL vials for 0, 3, 6, 12, and 24 min at 30°C. For the first series of aliquots, the incubations were terminated at each time point by addition of a CaCl$_2$/EDTA mixture as described above, and the resulting mixtures were analyzed for volatiles using SPME-GC-MS. The duplicate series of aliquots was extracted with 3 mL of formic acid:methanol (1:1,000, v/v) solution and subsequently analyzed for PhP volatile glycosides using LC-QTOF-MS as described in the corresponding sections above.

GC-MS Data Processing

The 94 volatile organic compound profiles derived using the SPME-GC-MS method were processed by the MetAlign software package (www.metalign.nl) for baseline correction, noise estimation, and ion-wise mass spectral alignment. The data matrix obtained was subjected to a fragment ion clustering for data size reduction and putative compound mass spectra extraction using the MMSR approach (Tikunov et al., 2005). The MMSR procedure was performed using a C++-based software package that was developed in-house. Each cluster in the reduced data set was represented by a single ion fragment (i.e. the most abundant fragment ion that reflected an average intensity pattern of an entire cluster [putative compound mass spectrum] derived by MMSR). The mass spectra of the clusters derived (number of fragment ions in a mass spectrum ≥ 5) were then subjected to a tentative identification using the National Institute of Standards and Technology mass spectral library (www.nist.gov).

LC-QTOF-MS Data Processing

Like the GC-MS profiles, the profiles derived by LC-QTOF-MS were processed by MetAlign software (at settings as described by Moco et al. [2006]), and the data set obtained was reduced using the MMSR approach. Similar to GC-MS data, the reduced LC-MS data consisted of single masses representative of an ion cluster (including isotopes, adducts, and fragments obtained by unintended in-source fragmentation). Also, ion fragments not correlating to any cluster by MMSR and with a maximum intensity of more than 200 counts per scan (a threshold for a reliable accurate mass calculation with our QTOF instrument) were manually added to the data matrix.

Data Normalization, Fusion, and Multivariate Analysis

Prior to fusion of the two data sets, the ion fragment intensities were normalized using log$_2$ transformation and standardized using range scaling, in which each value in a certain row, corresponding to a specific ion, was divided by the intensity range observed for this row throughout all samples analyzed (Smilde et al., 2005). Each row was then mean centered. Finally, both

data matrices were concatenated along the sample (genotype) dimension yielding a fused data matrix with normalized and log-transformed signal values. Principal components analysis implemented in GeneMath XT version 1.6 software (www.applied-maths.com) was used for unsupervised cluster analysis of the metabolites. Pearson's product-moment correlation coefficient was used as a measure for metabolite-metabolite correlation.

Supplemental Data

The following materials are available in the online version of this article.

Supplemental Table S1. Identification of tomato volatiles.

LITERATURE CITED

Baldwin EA, Scott JW, Einstein MA, Malundo TMM, Carr BT, Shewfelt RL, Tandon KS (1998) Relationship between sensory and instrumental analysis for tomato flavor. J Am Soc Hortic Sci **123:** 906–915

Baldwin EA, Scott JW, Shewmaker CK, Schuch W (2000) Flavor trivia and tomato aroma: biochemistry and possible mechanisms for control of important aroma components. HortScience **35:** 1013–1022

Baldwin IT, Halitschke R, Paschold A, Von Dahl CC, Preston CA (2006) Volatile signaling in plant-plant interactions: "talking trees" in the genomics era. Science **311:** 812–815

Bilia AR, Escudero Rubio MM, Alvares ML, Morelli M, Gonzalez JM (1994) New benzyl alcohol glycosides from Pyrus bourgaeana. Planta Med **60:** 569–571

Boatright J, Negre F, Chen X, Kish CM, Wood B, Peel G, Orlova I, Gang D, Rhodes D, Dudareva N (2004) Understanding in vivo benzenoid metabolism in petunia petal tissue. Plant Physiol **135:** 1993–2011

Bovy A, Schijlen E, Hall RD (2007) Metabolic engineering of flavonoids in tomato (Solanum lycopersicum): the potential for metabolomics. Metabolomics **3:** 399–412

Bovy AG, Gomez-Roldan V, Hall RD (2010) Strategies to optimize the flavonoid content of tomato fruit. In C Santos-Buelga, MT Escribano-Bailon, V Lattanzio, eds, Recent Advances in Polyphenol Research, Vol II. Blackwell Publishing, Oxford (in press)

Bowles D, Isayenkova J, Lim EK, Poppenberger B (2005) Glycosyltransferases: managers of small molecules. Curr Opin Plant Biol **8:** 254–263

Butelli E, Titta L, Giorgio M, Mock HP, Matros A, Peterek S, Schijlen EGWM, Hall RD, Bovy AG, Luo J, et al (2008) Enrichment of tomato fruit with health-promoting anthocyanins by expression of select transcription factors. Nat Biotechnol **26:** 1301–1308

Buttery RG, Ling LC (1993) Volatiles of tomato fruits and plant parts: relationship and biogenesis. In R Teranishi, RG Buttery, H Sugisawa, eds, Bioactive Volatile Compounds from Plants. ACS Books, Washington, DC, pp 23–24

Buttery RG, Takeoka G, Teranishi R, Ling LC (1990) Tomato aroma components: identification of glycoside hydrolysis volatiles. J Agric Food Chem **38:** 2050–2053

Buttery RG, Teranishi R, Ling LC (1987) Fresh tomato aroma volatiles: a quantitative study. J Agric Food Chem **35:** 540–544

Causse M, Saliba-Colombani V, Lecomte L, Duffe P, Rousselle P, Buret M (2002) QTL analysis of fruit quality in fresh market tomato: a few chromosome regions control the variation of sensory and instrumental traits. J Exp Bot **53:** 2089–2098

Chang SS, Kang DH (2004) Alicyclobacillus spp. in the fruit juice industry: history, characteristics, and current isolation/detection procedures. Crit Rev Microbiol **30:** 55–74

Crouzet J, Chassagne D (1999) Glycosidically bound volatiles in plants. *In* R Ikan, ed, Naturally Occurring Glycosides. John Wiley & Sons, Chichester, UK, pp 226–273

D'Auria JC (2006) Acyltransferases in plants: a good time to be BAHD. Curr Opin Plant Biol 9: 331–340

D'Auria JC, Reichelt M, Luck K, Svatos A, Gershenzon J (2007) Identification and characterization of the BAHD acyltransferase malonyl CoA: anthocyanidin 5-O-glucoside-6′′-O-malonyltransferase (At5MAT) in Arabidopsis thaliana. FEBS Lett 581: 872–878

Day JA, Saunders FM (2004) Glycosidation of chlorophenols by Lemna minor. Environ Toxicol Chem 23: 102–109

Dhaubhadel S, Farhangkhoee M, Chapman R (2008) Identification and characterization of isoflavonoid specific glycosyltransferase and malonyltransferase from soybean seeds. J Exp Bot 59: 981–994

Dudareva N, Negre F, Nagegowda DA, Orlova I (2006) Plant volatiles: recent advances and future perspectives. CRC Crit Rev Plant Sci 25: 417–440

Dudareva N, Pichersky E (2000) Biochemical and molecular genetic aspects of floral scents. Plant Physiol 122: 627–633

Dudareva N, Pichersky E, Gershenzon J (2004) Biochemistry of plant volatiles. Plant Physiol 135: 1893–1902

Forouhar F, Yang Y, Kumar D, Chen Y, Fridman E, Park SW, Chiang Y, Acton TB, Montelione GT, Pichersky E, et al (2005) Structural and biochemical studies identify tobacco SABP2 as a methyl salicylate esterase and implicate it in plant innate immunity. Proc Natl Acad Sci USA 102: 1773–1778

Gang DR (2005) Evolution of flavors and scents. Annu Rev Plant Biol 56: 301–325

Gavai AK, Tikunov Y, Ursem R, Bovy A, van Eeuwijk F, Nijveen H, Lucas PJF, Leunissen JAM (2009) Constraint-based probabilistic learning of metabolic pathways from tomato volatiles. Metabolomics (in press)

Goff SA, Klee HJ (2006) Plant volatile compounds: sensory cues for health and nutritional value? Science 311: 815–819

Herderich M, Feser W, Schreier P (1992) Vomifoliol 9-O-beta-D-glucopyranosyl-4-O-beta-D-xylopyranosyl-6-O-beta-D-glucopyranoside: a trisaccharide glycoside from apple fruit. Phytochemistry 31: 895–897

Kappers IF, Aharoni A, Van Herpen TWJM, Luckerhoff LLP, Dicke M, Bouwmeester HJ (2005) Plant science: genetic engineering of terpenoid metabolism attracts bodyguards to Arabidopsis. Science 309: 2070–2072

Kazuma K, Noda N, Suzuki M (2003) Malonylated flavonol glycosides from the petals of Clitoria ternatea. Phytochemistry 62: 229–237

Kijima H, Ide T, Otsuka H, Ogimi C, Hirata E, Takushi A, Takeda Y (1997) Water-soluble phenolic glycosides from leaves of Alangium premnifolium. Phytochemistry 44: 1551–1557

Koeduka T, Fridman E, Gang DR, Vassao DG, Jackson BL, Kish CM, Orlova I, Spassova SM, Lewis NG, Noel JP, et al (2006) Eugenol and isoeugenol, characteristic aromatic constituents of spices, are biosynthesized via reduction of a coniferyl alcohol ester. Proc Natl Acad Sci USA 103: 10128–10133

Kogawa K, Kazuma K, Kato N, Noda N, Suzuki M (2007) Biosynthesis of malonylated flavonoid glycosides on the basis of malonyltransferase activity in the petals of Clitoria ternatea. J Plant Physiol 164: 886–894

Kovács K, Fray RG, Tikunov Y, Graham N, Bradley G, Seymour GB, Bovy AG, Grierson D (2009) Effect of tomato pleiotropic ripening mutations on flavour volatile biosynthesis. Phytochemistry 70: 1003–1008

Krumbein A, Auerswald H (1998) Characterization of aroma volatiles in tomatoes by sensory analyses. Nahrung 42: 395–399

Krumbein A, Peters P, Bruckner B (2004) Flavour compounds and a quantitative descriptive analysis of tomatoes (Lycopersicon esculentum Mill.) of different cultivars in short-term storage. Postharvest Biol Technol 32: 15–28

Marlatt C, Ho CT, Chien M (1992) Studies of aroma constituents bound as glycosides in tomato. J Agric Food Chem 40: 249–252

Mizutani M, Nakanishi H, Ema J, Ma SJ, Noguchi E, Inohara-Ochiai M, Fukuchi-Mizutani M, Nakao M, Sakata K (2002) Cloning of β-primeverosidase from tea leaves, a key enzyme in tea aroma formation. Plant Physiol 130: 2164–2176

Moco S, Bino RJ, Vorst O, Verhoeven HA, De Groot J, Van Beek TA, Vervoort J, De Vos RCH (2006) A liquid chromatography-mass spectrometry-based metabolome database for tomato. Plant Physiol 141: 1205–1218

Moco S, Capanoglu E, Tikunov Y, Bino RJ, Boyacioglu D, Hall RD, Vervoort J, De Vos RCH (2007) Tissue specialization at the metabolite level is perceived during the development of tomato fruit. J Exp Bot 58: 4131–4146

Ortiz-Serrano P, Gil JV (2007) Quantitation of free and glycosidically bound volatiles in and effect of glycosidase addition on three tomato varieties (Solanum lycopersicum L.). J Agric Food Chem 55: 9170–9176

Park SW, Kaimoyo E, Kumar D, Mosher S, Klessig DF (2007) Methyl salicylate is a critical mobile signal for plant systemic acquired resistance. Science 318: 113–116

Petro-Turza M (1987) Flavour of tomato and tomato products. Food Rev Int 2: 309–351

Ruiz JJ, Alonso A, Garcia-Martinez S, Valero M, Blasco P, Ruiz-Bevia F (2005) Quantitative analysis of flavour volatiles detects differences among closely related traditional cultivars of tomato. J Sci Food Agric 85: 54–60

Sasso R, Iodice L, Digilio MC, Carretta A, Ariati L, Guerrieri E (2007) Host-locating response by the aphid parasitoid Aphidius ervi to tomato plant volatiles. J Plant Interact 2: 175–183

Schijlen EGWM, Beekwilder J, Hall RD, van der Meer IM (2008) Boosting beneficial phytochemicals in vegetable crop plants. CAB Rev 3: 1–21

Schwab W, Davidovich-Rikanati R, Lewinsohn E (2008) Biosynthesis of plant-derived flavor compounds. Plant J 54: 712–732

Shulaev V, Silverman P, Raskin I (1997) Airborne signalling by methyl salicylate in plant pathogen resistance. Nature 385: 718–721

Smilde AK, Van Der Werf MJ, Bijlsma S, Van Der Werff-Van Der Vat BJC, Jellema RH (2005) Fusion of mass spectrometry-based metabolomics data. Anal Chem 77: 6729–6736

Suzuki H, Nishino T, Nakayama T (2007) cDNA cloning of a BAHD acyltransferase from soybean (Glycine max): isoflavone 7-O-glucoside-6′′-O-malonyltransferase. Phytochemistry 68: 2035–2042

Tandon KS, Baldwin EA, Shewfelt RL (2000) Aroma perception of individual volatile compounds in fresh tomatoes (Lycopersicon esculentum, Mill.) as affected by the medium of evaluation. Postharvest Biol Technol 20: 261–268

Tieman DM, Zeigler M, Schmelz EA, Taylor MG, Bliss P, Kirst M, Klee HJ (2006) Identification of loci affecting flavour volatile emissions in tomato fruits. J Exp Bot 57: 887–896

Tikunov Y, De Vos RCH, Verhoeven HA, Bino RJ, Hall RD, Bovy AG (2005) A novel approach for nontargeted data analysis for metabolomics: large-scale profiling of tomato fruit volatiles. Plant Physiol 139: 1125–1137

Tikunov YM, Verstappen FW, Hall RD (2007) Metabolomic profiling of natural volatiles: headspace trapping: GC-MS. Methods Mol Biol 358: 39–53

Unno H, Ichimaida F, Suzuki H, Takahashi S, Tanaka Y, Saito A, Nishino T, Kusunoki M, Nakayama T (2007) Structural and mutational studies of anthocyanin malonyltransferases establish the features of BAHD enzyme catalysis. J Biol Chem 282: 15812–15822

Ursem R, Tikunov Y, Bovy A, Van Berloo R, Van Eeuwijk F (2008) A correlation network approach to metabolic data analysis for tomato fruits. Euphytica 161: 181–193

Van Berloo R, Zhu A, Ursem R, Verbakel H, Gort G, Van Eeuwijk FA (2008) Diversity and linkage disequilibrium analysis within a selected set of cultivated tomatoes. Theor Appl Genet 117: 89–101

Wildermuth MC, Dewdney J, Wu G, Ausubel FM (2001) Isochorismate synthase is required to synthesize salicylic acid for plant defence. Nature 414: 562–565

Withopf B, Richling E, Roscher R, Schwab W, Schreier P (1997) Sensitive and selective screening for 6′-O-malonylated glucoconjugates in plants. J Agric Food Chem 45: 907–911

Zanor MI, Rambla JL, Chaib J, Steppa A, Medina A, Granell A, Fernie AR, Causse M (2009) Metabolic characterization of loci affecting sensory attributes in tomato allows an assessment of the influence of the levels of primary metabolites and volatile organic contents. J Exp Bot 60: 2139–2154